Heterogeneous versus homogeneous nucleation of kink-antikink pairs

Thomas Christen
Institut für Theoretische Physik, Universität Basel, Klingelbergstrasse 82, CH-4056 Basel, Switzerland
(Received 27 July 1994)

Under the influence of noise, metastable states in spatially one-dimensional systems decay via nucleation of kink-antikink pairs. In a realistic sample, translational invariance is destroyed by the finite size of the sample and by the presence of localized impurities. This leads to a competition between homogeneous and heterogeneous nucleation, i.e., the generation of free kink-antikink pairs in the bulk and kink-antikink pairs pinned at the sample surface or at impurities. For systems that can be modeled by a bistable reaction-diffusion equation, we derive the rates of homogeneous and heterogeneous nucleation in the framework of Kramers theory. In particular, the critical sample length and the critical density of impurities associated with the crossover between qualitatively different types of nucleation are derived. The results concerning the crossover density of impurities turn out to depend strongly on how the impurities couple to the order-parameter field.

PACS number(s): 82.60.Nh, 05.40.+j, 05.70.Ln

I. INTRODUCTION

The decay of linearly but not globally stable states in spatially extended noisy systems is of interest in many respects. For example, maintaining a supersaturated state during a given time requires a sufficiently low noise level the knowledge of which can be of technical use. On the other hand, the presence of a sufficiently strong noise source is often necessary in order to accelerate processes which are inhibited by activation barriers. Prominent examples are the nucleation problem at first-order phase transitions [1], chemical reaction rates of processes including activated intermediate states [2,3], and the nucleation of dissipative structures such as, e.g., current filaments in certain nonlinear semiconductors [4,5], to mention only a few. These and many other systems of these kinds in physics, chemistry, and biology are frequently modeled by multistable reaction-diffusion equations supplemented by a weak white-noise force [6,7]. Here, multistability refers to the existence of a set of linearly stable stationary states. Once a system is prepared in such a state, every small perturbation decays to zero, and a certain *finite* perturbation has to be applied in order to escape from the basin of attraction. For example, the decay of metastable states in equilibrium systems requires an excitation called the "critical nucleus" with finite activation energy ΔE. States beyond this lowest saddle state expand whereby the more stable phase is established. Whereas a linearly unstable state decays *immediately* due to the growth of infinitesimal fluctuations, the very small probability of a finite fluctuation implies a *large* time scale of the nucleation processes.

We will consider a spatially one-dimensional reaction-diffusion equation for a real one-component order parameter. This system possesses a Lyapunov functional (energy functional) so that standard Kramers theory can be applied [1,8–10]; effects based on the fact that generic nonequilibrium systems are nonvariational will not be considered (see, e.g., [11]). The nucleation rate can be expressed by the Arrhenius factor $\exp(-\beta\Delta E)$ with the activation energy ΔE and the noise strength β^{-1}, and a prefactor containing the curvatures of the energy surface in function space at the metastable and the activated state, as well as the number of equivalent saddles. Note that the lowest saddle state has one *single* negative curvature associated with the growth rate of the unstable mode. In reaction-diffusion equations with one spatial coordinate the saddle corresponds to a stationary kink-antikink pair (KAP) with an unstable amplitude mode. A lot of work has already been done concerning the nucleation of KAP's in *homogeneous* samples (for a review, see Ref. [8]). In particular, the nucleation rate has been studied for the different limits of the weakly and strongly supersaturated states and also for the nondiffusive case including many-body effects of KAP's [12,13].

Due to the existence of a Goldstone mode associated with translational invariance the prefactor is proportional to the sample length L; thus, as one expects, the rate is an extensive quantity [1,9]. In realistic samples, however, translational invariance is violated by the finiteness of the sample extensions and by the existence of impurities, giving rise to heterogeneous nucleation of a KAP at these inhomogeneities in contrast to homogeneous nucleation of a free KAP in the uniform bulk. Depending on the explicit form of the boundary conditions the nucleation of a KAP at a boundary can be favored if the activation energy is lower than in the bulk. In that case, there must be a characteristic sample length L_c below which boundary nucleation is preferred. Note that if the bulk is a "powder" composed of independent uniform grains, L_c^{-1} can be interpreted as a density of grains associated with the crossover between homogeneous and heterogeneous nucleation of KAP's at grain boundaries. Similarly, a localized pinning impurity [14] which lowers the activation energy can act as a nucleation center, and one expects the existence of a characteristic density of impurities ρ_{im}^{c} associated with the crossover from homogeneous to heterogeneous nucleation.

The aim of this paper is the derivation and the discussion of the rates r_f, r_b, and $r_{\rm im}$ of free, boundary sustained, and impurity sustained, nucleation of KAP's, respectively. The considerations will be restricted to a strongly supersaturated metastable state where the critical nucleus is a strongly interacting KAP. Furthermore, an interaction of different KAP's will be neglected, and a dilute density of impurities will be assumed. We will not enter into the question about the dynamics of the state after an expanding domain of the globally stable phase has formed; we only recall the well-known fact that in a homogeneous sample a domain wall propagates into the less stable state with a velocity approximately proportional to the difference between the energy densities of the states separated by the wall [15]. Although for sufficiently weak impurity forces the dynamics of the KAP could be described in terms of collective coordinates corresponding to the location of the kinks [16,17], to deal with the general case of arbitrary impurity forces would require more sophisticated methods.

In Sec. II, the model is introduced: it is a one-dimensional bistable reaction-diffusion equation with a piecewise linear nonlinearity. Compared to the frequently used overdamped sine-Gordon equation or the Ginzburg-Landau equation with polynomial nonlinearities, this model has the advantage that analytical results are accessible. In Sec. III, the strongly supersaturated metastable and the activated state are discussed. The nucleation rates are derived in Sec. IV, and in Sec. V the sample length L_c and the density $\rho_{\rm im}^c$ associated with the crossover between homogeneous and heterogeneous nucleation are obtained. In Sec. VI, the results are illustrated by two examples of different impurities, one type with an impurity force independent of the order-parameter field and another one where the field is coupled back to the impurity.

II. THE MODEL

We consider a system the state of which is described by the one-component order-parameter field $\phi(x,t)$ obeying the dimensionless, spatially one-dimensional reaction-diffusion equation

$$\partial_t\phi = \partial_x^2\phi + g - f(\phi) + \sum_j \delta(x-a_j)F(\phi) + \xi(x,t) \ . \tag{1}$$

The control parameter is denoted by g, and the nonlinearity $f(\phi)$ is modeled by the continuous and piecewise linear function (Fig. 1)

$$f(\phi) = \begin{cases} q^{-2}\phi, & \phi < 0 \ , \\ -\phi, & 0 \le \phi \le 1 \ , \\ p^{-2}\phi - (1+p^{-2}), & 1 < \phi \ , \end{cases} \tag{2}$$

where p^2 and q^2 are ratios of characteristic time scales. The order parameter is assumed to satisfy homogeneous Neumann boundary conditions (i.e., $\partial_x\phi|_{\pm L/2} = 0$) at the sample boundaries $\pm L/2$. The sum of the weighted Dirac δ functions on the right-hand side (RHS) of Eq. (1) describes the action of pointlike impurities located at a_j. The associated inverse density of impurities, $\rho_{\rm im}^{-1}$, and the length L of the sample, are assumed to be much larger than any characteristic intrinsic length, hence $L, \rho_{\rm im}^{-1} \gg \max\{1,q,p\}$. The force $F(\phi) \equiv -U'(\phi)$ of a single impurity acting on the order-parameter field is related to a potential $U(\phi)$ by differentiation, which is denoted by the prime; specific examples of potentials $U(\phi)$ will be given in Sec. VI. The small density of impurities will allow us to neglect the interaction of the critical nucleus with more than one impurity, and we will consider a single impurity located at $x = 0$ for the calculations in Sec. III. The last expression $\xi(x,t)$ in Eq. (1) represents a weak white-noise force with vanishing expectation value and δ-function correlation $\langle\xi(x,t)\rangle = 0$ and

$$\langle\xi(x,t)\xi(\tilde{x},\tilde{t})\rangle = (2/\beta)\delta(x-\tilde{x})\delta(t-\tilde{t}) \ , \tag{3}$$

where $\beta \gg 1$. If one deals with equilibrium systems, noise refers to thermal fluctuations obeying $\beta^{-1} = kT$, where k and T are Boltzmann's constant and the temperature of the heat bath coupled to the order-parameter field, respectively.

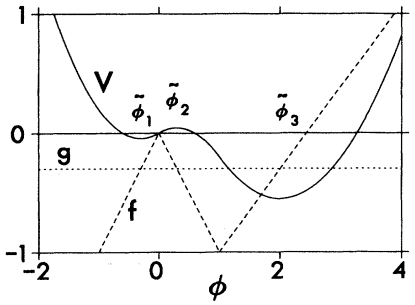

FIG. 1. The stationary uniform states $(\tilde{\phi}_1, \tilde{\phi}_2, \tilde{\phi}_3)$ of the sample without impurity are given by the intersection points of $f(\phi)$ (dashed) with g (dotted) and correspond to the extrema of the potential $V(\phi)$ (solid).

The evolution equation (1) can be expressed in terms of a Lyapunov functional $E[\phi]$ by

$$\partial_t\phi = -\frac{\delta E[\phi]}{\delta\phi} + \xi(x,t) \ . \tag{4}$$

In the following we call

$$E[\phi] = \int_{-L/2}^{L/2} dx \left(\frac{1}{2}(\partial_x\phi)^2 + V(\phi)\right) + \sum_j U(\phi(a_j)) \tag{5}$$

the energy of the state ϕ. One verifies that the continuous density

$$V(\phi) = \begin{cases} \phi^2/2q^2 - g\phi, & \phi < 0 \\ -\phi^2/2 - g\phi, & 0 \le \phi \le 1 \\ (1+p^{-2})(1/2-\phi) + \phi^2/2p^2 - g\phi, & 1 < \phi \end{cases} \tag{6}$$

leads to $f(\phi)$ of Eq. (2). The potential density $V(\phi)$ is shown in Fig. 1. States that are independent of time

correspond to stationary points of the energy, the minima of which are stable. While the deterministic behavior is a relaxation to a local minimum for nearby initial conditions ($\partial_t E \leq 0$), the fluctuating force ξ drives a metastable state of the dissipative system (4) via activated states towards the global minimum of the energy. Before deriving the characteristic time scale of this process, the metastable and the activated states have to be determined and some of their properties must be discussed.

III. THE METASTABLE AND THE ACTIVATED STATES

Consider first a uniform sample void of any impurity (i.e., $F \equiv 0$). Stationary uniform solutions are then given by

$$\phi = \begin{cases} \tilde{\phi}_1 \equiv q^2 g, & g < 0 \ , \\ \tilde{\phi}_2 \equiv -g, & -1 \leq g \leq 0 \ , \\ \tilde{\phi}_3 \equiv p^2 g + (1+p^2), & -1 < g \ . \end{cases} \tag{7}$$

At $g = 0$ and $g = -1$ cusp-shaped saddle-node bifurcations of uniform states occur (see Fig. 1). Linear stability analysis shows that $\tilde{\phi}_2$ is linearly unstable and $\tilde{\phi}_1$, $\tilde{\phi}_3$ are linearly stable. Thus, in the range $-1 < g < 0$ there occurs bistability of uniform states that are the minima of the double-well-shaped potential $V(\phi)$. The value $g_{\rm eq}$ of the control parameter where $\tilde{\phi}_1$ and $\tilde{\phi}_3$ have equal energy density is given by

$$g_{\rm eq} \equiv -\left[1 + \sqrt{(1+q^2)/(1+p^2)}\right]^{-1} \ . \tag{8}$$

Therefore, $\tilde{\phi}_1$ is metastable if $g_{\rm eq} < g < 0$ and will decay under the influence of noise via the nucleation of a KAP. The restriction to the strongly supersaturated state means that the case $g \approx g_{\rm eq}$ will not be considered.

Let us first concentrate on localized bulk states located far away from the sample boundaries. Since the stationary Eq. (1) is formally equivalent to the equation of motion of a classical particle in a one-dimensional potential with two hills [15], the stationary solutions can be illustrated in the phase plane $(\phi, \partial_x \phi)$ as shown in Fig. 2. The solid curves are the trajectories connected to the hyperbolic fixed point $\tilde{\phi}_1$. The latter corresponds to the metastable state, and the single-humped solution $\phi(x)$ of Eq. (1) given by the homoclinic trajectory corresponds to the nucleus. Since the nucleus is not restricted to a certain place in the sample, it will be called the "free (critical) nucleus."

For finite impurity force (i.e., $F \not\equiv 0$), on the other hand, it depends on the explicit form of $F(\phi)$ how many

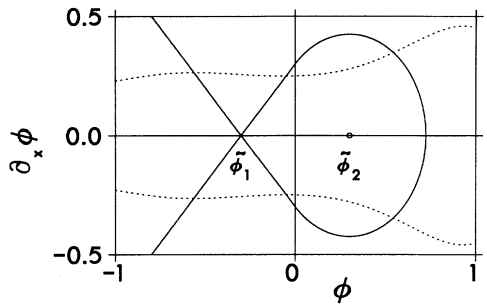

FIG. 2. Phase plane $(\phi, \partial_x \phi)$ associated with the stationary Eq. (1). $F(\phi) \equiv 0$: the metastable state $\tilde{\phi}_1$ and the critical nucleus correspond to the hyperbolic fixed point and to the homoclinic curve (solid), respectively. $F(\phi) \not\equiv 0$: solutions belong to orbits in the phase plane starting from $x = \pm\infty$ at the hyperbolic fixed point $\phi = \tilde{\phi}_1$ and ending at $x = \pm 0$ with a value of ϕ obtained from the intersection of the orbits (solid) with the curves $\mp F(\phi)/2$ (dotted).

different stationary solutions representing candidates for the saddles exist. First, the free nucleus $\phi(x - x_0)$ is still a solution if it is located at a place x_0 such that $F(\phi(-x_0)) = 0$ holds. Secondly, a finite value of $F(\phi)$ at the impurity ($x = 0$) implies a finite jump of the derivative: $\partial_x \phi(0^+) - \partial_x \phi(0^-) = -F(\phi(0))$ (self-consistency condition). In this case, the solution can be constructed by plotting the functions $\pm F(\phi)/2$ in the phase plane and matching those parts of the trajectories which start at their intersection point with $\pm F(\phi(0))/2$ at $x = 0$ and end at $\tilde{\phi}_1$ for $x = \mp\infty$ (see Fig. 2). Obviously, this construction satisfies the self-consistency condition and the requirement of the continuity of the solution. We will restrict the investigations in the following to the second case where the relevant saddle (i.e., having the lowest energy among saddle solutions) is symmetric at the impurity. The further restriction to the strongly supersaturated metastable state will be accomplished by the limitation to the case where a free critical nucleus satisfies $\phi(0) < 1$; an equivalent condition for g will be given below. For the sake of clarity, we will use the abbreviations $F \equiv F(\phi(0))$, $U \equiv U(\phi(0))$, $F' \equiv F'(\phi(0))$.

If $\phi(0) \leq 0$, the localized state is given by

$$\phi(x) = \tilde{\phi}_1 + [\phi(0) - \tilde{\phi}_1] \exp(-|x|/q) \ , \tag{9}$$

where terms of $O(\exp\{-L/q\})$ have been neglected. The amplitude $\phi(0)$ is determined by the self-consistency condition $\phi(0) = \tilde{\phi}_1 + qF/2$, and the requirement $\phi(0) \leq 0$ implies $F < -2qg$. The stationary single-humped state satisfying $0 < \phi(0) < 1$ and $\phi(x) \to \tilde{\phi}_1$ for large $|x|$ is given by

$$\phi(x) = \begin{cases} \tilde{\phi}_2 + \hat{\phi}_2 \cos(x) - (F/2)\sin(|x|), & |x| \leq x_{\rm im} \ , \\ \tilde{\phi}_1 \left[1 - \exp\{(x_{\rm im} - |x|)/q\}\right], & x_{\rm im} < |x| \ , \end{cases} \tag{10}$$

where again terms of $O(\exp\{-L/q\})$ have been neglected. The states given by Eqs. (9) and (10) are shown in Fig. 3 for various values of F. The condition $\phi(x_{\rm im}) = 0$ and the differentiability of $\phi(x)$ at $x_{\rm im}$ imply

$$F = F_c \sin(x_f - x_{\rm im}) \ , \tag{11}$$

where

$$F_c \equiv -2g\sqrt{1+q^2} \tag{12}$$

is a critical value of the force which will be discussed below. Equation (11) provides the size $2x_{\rm im}$ of the localized state, where $0 \le x_{\rm im} \le x_f + \pi$ with $x_f = \pi - \arctan(q)$ being half of the size of the free critical nucleus (see Fig. 3). The self-consistency condition reads

$$(\hat{\phi}_2)^2 = \frac{1}{4}(F_c^2 - F^2) \ , \tag{13}$$

where F depends on the amplitude $\phi(0) = \tilde{\phi}_2 + \hat{\phi}_2$ of the critical nucleus.

One finds that for the free critical nucleus the restriction $\phi(0) < 1$ requires

$$g > g_1 \equiv -\left(1 + \sqrt{1+q^2}\right)^{-1} \ , \tag{14}$$

where $x_{\rm im} = x_f$ is independent of the control parameter g, and where the amplitude $\phi(0) = \tilde{\phi}_2 + F_c$ shrinks linearly with g. The stability eigenvalue problem of the nonuniform state against perturbations of the form $\delta\phi \propto \exp(\lambda t)$ turns out to be equivalent to the determination of the quantum-mechanical energy eigenvalues of a particle in a one-dimensional rectangular potential well. For systems of the type of Eq. (1), it can be shown that a free single-humped state is unstable against a symmetric amplitude mode [4,18]. Due to translational symmetry in the limit of infinite sample length L, there exists a second non-negative eigenvalue which vanishes and indicates the existence of the Goldstone mode $\partial_x\phi$. For finite but still large L this eigenvalue is shifted by an amount λ_B of $O(\exp\{-L/q\})$ which can be understood as the growth rate arising from the interaction of the localized structure [16,17] with its mirror images at the sample boundaries.

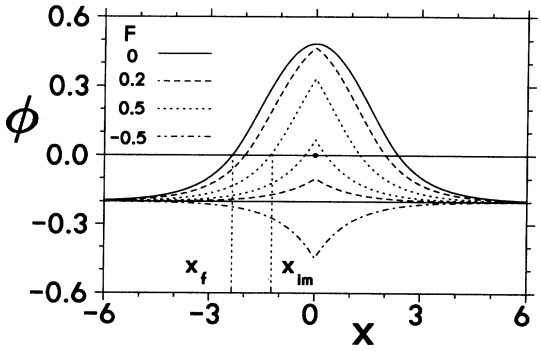

FIG. 3. Stationary solutions (metastable states and saddles) $\phi(x)$ for some values of the impurity force F ($q = 1$, $g = -0.2$).

All the other stability eigenvalues are negative and thus belong to damped modes. In order to derive λ_B by stability analysis, one has to linearize Eq. (1) at the exact solution satisfying the boundary conditions at $x = \pm L$. One finds for large L

$$\lambda_B = \frac{8qg^2}{||\partial_x\phi||^2} \exp\{(2x_f - L)/q\} \ , \tag{15}$$

where the denominator equals the activation energy $\Delta E[\phi] = E[\phi] - E[\tilde{\phi}_1]$ of the free critical nucleus (index f)

$$\Delta E_f = ||\partial_x\phi||^2 \equiv \int_{-L/2}^{L/2} dx \ (\partial_x\phi)^2 = \frac{(x_f + q)}{4} F_c^2 \ . \tag{16}$$

The exponentially small shift λ_B of the zero eigenvalue causes an extremely slow drift of the critical nucleus. Since the time scale of this motion is much larger than any other relevant time this shift will be neglected in the following.

Next, we note that the localized surface states follow directly from the free bulk nucleus. Indeed, if the localized bulk solution $\phi(x - x_0)$ is centered at a boundary (i.e., $x_0 = \pm L/2$) the resulting state satisfies the boundary conditions and provides a stationary solution of Eq. (1) possessing only half of the activation energy compared to a free critical nucleus in the bulk. It follows from the Neumann boundary conditions that this surface state describing a kink pinned at a boundary is a saddle since eigenvalues of even eigenfunctions remain the same as for the bulk nucleus but odd eigenfunctions do not occur.

Consider now an impurity with small $|F/F_c|$. The main effect of the weak impurity force destroying translational symmetry is again expected to be a small shift $\lambda_{\rm pin}$ of the former zero eigenvalue. One can approximate $\lambda_{\rm pin}$ by using a collective-coordinate ansatz [16,17]. Projecting Eq. (1) onto the Goldstone mode $\partial_x\phi$ of the free localized state $\phi(x - x_0(t))$ at x_0 leads to a differential equation for x_0. Linearization of the dynamics at the stationary state $x_0 = 0$ yields the growth rate

$$\lambda_{\rm pin} = -\frac{2}{x_f + q} \frac{F}{F_c} + O\left(\left(\frac{F}{F_c}\right)^2\right) \ . \tag{17}$$

In order that $\phi(x)$ is a saddle with a single unstable direction, $F > 0$ is required which is equivalent to a pinning impurity. ("Pinning" refers here to the stabilization of the translational mode.) Equation (11) then implies $x_{\rm im} < x_f$ reflecting the contraction of the pinned nucleus. If $0 < F < -2qg$, a single solution $x_{\rm im}^s$ with $0 < x_{\rm im}^s < x_f$ belonging to the positive sign in Eq. (13) exists; for $F_c > F > -2qg$ an additional solution $x_{\rm im}^m$ of Eq. (11) exists, associated with the negative sign in Eq. (13) (see Fig. 4 below). At the critical value F_c of a constant impurity force the metastable state and the saddle merge at a saddle-node bifurcation. This implies a lowering of the bifurcation point $g_c = 0$ by a general impurity force, provided $F(0) \neq 0$ (see Fig. 5 below). Note that for negative values of the impurity force [e.g.,

for odd $F(\phi)$] metastable states exist and are associated with the nonhomoclinic orbits connected to $\tilde{\phi}_1$ in Fig. 2 ($F = -0.5$ in Fig. 3).

From the above mentioned equivalent Schrödinger problem one finds that the stability eigenvalue $\lambda_s^{(0)}$ of the unstable breathing mode is given by the largest real solution of

$$\sqrt{1-\lambda}\left(\sqrt{\lambda+q^{-2}}-F'/2\right) - \left(\sqrt{\lambda+q^{-2}}\,F'/2+\ 1-\lambda\ \right)\tan(\sqrt{1-\lambda}\,x_{\rm im}) = 0\ , \tag{18}$$

and the eigenvalue $\lambda_s^{(1)}$ ($\equiv \lambda_{\rm pin}$) associated with the first antisymmetric mode is given by the largest real solution of

$$\sqrt{1-\lambda}+\sqrt{\lambda+q^{-2}}\tan(\sqrt{1-\lambda}\,x_{\rm im}) \times \tanh\left[\sqrt{\lambda+q^{-2}}(L/2-x_{\rm im})\right] = 0\ . \tag{19}$$

If $F \equiv 0$ (i.e., $x_{\rm im} \equiv x_f$), one finds again that $\lambda_s^{(1)}$ goes to zero for $L \to \infty$. We mention that it is necessary to consider the term $\tanh(\cdots)$ in Eq. (19) for strong forces where $\lambda_s^{(1)} < -q^{-2}$ belongs to the quasicontinuous spectrum. Equations (18) and (19) further imply that an attractive impurity causes a negative shift of $\lambda_s^{(1)}$ but not necessarily of $\lambda_s^{(0)}$ (see Fig. 6 below). In the following, the other eigenvalues $\lambda_{m,s}^{(n)}$ ($n > 1$) will not be needed explicitly and will thus not be specified.

From Eq. (5) one obtains the change of the activation energy caused by an impurity:

$$\Delta E_{\rm im} = U_s - U_m + \frac{1}{4}F_c^2(x_{\rm im}^s - x_f) + \frac{1}{2}[\phi_s(0)-\tilde{\phi}_2]F_s - \frac{1}{2}[\phi_m(0)-\tilde{\phi}_1]F_m\ , \tag{20}$$

where the indices m and s indicate the metastable and the saddle state corresponding to Eqs. (9) and (10), respectively. In the limit of a very small impurity force, Eq. (20) reduces simply to $\Delta E_{\rm im} \approx U_s - U_m$ where the potentials $U(\phi)$ are taken at the solutions $\phi_{m,s}$ for $F \equiv 0$. Equation (20) holds for $F_m < -2qg$; otherwise, if $-2qg < F_m < F_c$ the additional term $-F_c^2\left[x_{\rm im}^m + q + (F_m/2g)\right]/4$ must be added to the RHS of Eq. (20). The total activation energy consists of a sum of ΔE_f and $\Delta E_{\rm im}$ given by Eqs. (16) and (20), respectively:

$$\Delta E = \Delta E_f + \Delta E_{\rm im}\ . \tag{21}$$

Clearly, impurities serving as nucleation centers contribute with a negative $\Delta E_{\rm im}$.

IV. NUCLEATION RATES

Now we want to determine the escape rate from the metastable state, or, equivalently, the inverse time needed to cross the energy barrier in the presence of weak white noise. A common definition of the nucleation rate r is given by the ratio of the probability flux j across the saddle and the probability n to be in the metastable well, $r = j/n$ ("flux over population;" see, e.g., [8]). In the framework of Kramers theory the rate r in the system with many degrees of freedom given by Eq. (1) becomes [1,8–10]

$$r = \frac{\lambda_s^{(0)}}{2\pi}Se^{-\beta\Delta E}\ , \tag{22}$$

where the prefactor in front of the Arrhenius term is the product of the *dynamic prefactor* $\lambda_s^{(0)}/2\pi$ and the *static prefactor* S. The former is characterized by the growth rate $\lambda_s^{(0)} > 0$ of the unstable mode at the saddle. The static prefactor is given by

$$S = \sqrt{\frac{\prod_n(-\lambda_m^{(n)}\beta/2\pi)}{\left|\prod_n(-\lambda_s^{(n)}\beta/2\pi)\right|}}\ , \tag{23}$$

and contains the eigenvalues $\lambda_{m,s}^{(n)}$ of the stability eigenvalue problem of the metastable solution and of the critical nucleus, respectively. It must be emphasized that Kramers theory fails close to the saddle-node bifurcation where $\beta\Delta E \to 0$, and where therefore the following results are not correct.

The factors $\sqrt{-2\pi/\beta\lambda^{(n)}}$ in Eq. (23) arise from a Gaussian approximation of the partition function close to the stationary points of the energy. If there exists a discrete symmetry giving rise to N equivalent saddles, the static prefactor S must be replaced by NS. In the case of translational invariance the localized nucleus $\phi(x)$ breaks this continuous symmetry, implying the existence of a continuous manifold of equivalent saddles. Due to the existence of a Goldstone mode with vanishing eigenvalue the Gaussian approximation cannot be applied in this direction of the function space, and the integration must be performed more carefully. One can show that the exponentially diverging factor $\sqrt{-2\pi/\beta\lambda_B}$ in Eq. (23) must be replaced by the "volume of the translation group in function space"

$$\tilde{V} = L\,||\partial_x\phi||\ , \tag{24}$$

through which the rate becomes proportional to the length L of the sample [1,9,12].

We proceed now by sketching the derivation of the static prefactor S by using well-known field-theoretical techniques concerning the ratio of determinants of linear operators in Hilbert space [19]. In order to obtain an analytical expression one constructs from the stability eigenvalue problem analytical functions $D_{m,s}(\lambda)$ of the complex variable λ with the following properties [20]. First, their zeros are the eigenvalues $\lambda_{m,s}^{(n)}$, $n = 0, 1, \ldots$. Secondly, the order of these zeros is equal to the multiplicity (which equals unity in the present case) of the corresponding eigenvalues. Thirdly, they are normalized in the sense that $\lim_{|\lambda|\to\infty} D_m(\lambda)/D_s(\lambda) = 1$ (except on

the real line). From the uniqueness of a meromorphic function on the complex sphere if the poles, the zeros, and a single regular value are known, it follows that

$$\frac{D_m(\lambda)}{D_s(\lambda)} \equiv \frac{\prod_n(\lambda-\lambda_m^{(n)})}{\prod_n(\lambda-\lambda_s^{(n)})} \ . \tag{25}$$

Consequently, if there is no zero eigenvalue the static prefactor can be expressed as

$$S = \sqrt{-D_m(0)/D_s(0)} \ . \tag{26}$$

As mentioned above, the determination of the stability eigenvalues turns out to be equivalent to the problem of a quantum particle in a one-dimensional rectangular potential well. Solving this Schrödinger problem leads to the functions $D(\lambda)$ which finally have to be normalized. This procedure is straightforward and will not be carried out here in detail.

First, we give the result for the nucleation rate of a free KAP in the homogeneous bulk. It turns out that for large L

$$\frac{D_m(0)}{D_s(0)} = \frac{1}{4\exp(-L/q)} \ . \tag{27}$$

Clearly, the exponentially diverging ratio (27) for $L \to \infty$ indicates the existence of the zero eigenvalue associated with translational invariance. As remarked above, λ_B contained in $D_m(0)$ must be eliminated; by using Eqs. (15) and (24) one obtains (see also Ref. [20])

$$S_f = L||\partial_x\phi||\sqrt{\frac{\beta\lambda_B}{2\pi}\frac{D_m(0)}{D_s(0)}} = L\sqrt{\frac{\beta q g^2}{\pi}}\exp(x_f/q) \ . \tag{28}$$

Hence the nucleation rate of a free KAP can be written as

$$r_f = L\,\frac{\lambda_f}{2\pi}\,\chi(q)\,\sqrt{\beta\Delta E_f}\exp(-\beta\Delta E_f) \ , \tag{29}$$

where λ_f is the positive solution of Eq. (18) for $F \equiv 0$, and

$$\chi(q) = \sqrt{\frac{q}{\pi(1+q^2)(x_f+q)}}\exp(x_f/q) \ . \tag{30}$$

The result Eq. (29) is of the form of the rate given in Ref. [12]. The strong growth of the rate for $q \to 0$ is a consequence of the metastable potential well being extremely narrow in this limit.

In the same way, one obtains from Eqs. (22) and (26) the nucleation rate r_b of a kink at the surface, where now the antikink corresponds to the mirror image at the boundary. Taking into account that antisymmetric eigenfunctions do not appear, one finds

$$\frac{D_m(0)}{D_s(0)} = \frac{-1}{\sqrt{1+q^2}\exp(-x_f/q)} \ . \tag{31}$$

Since the activation energy equals one half of the value compared to the bulk case [see Eq. (16)], one finally obtains

$$r_b = 2\,\frac{\lambda_f}{2\pi}\sqrt{\frac{\exp(x_f/q)}{\sqrt{1+q^2}}}\exp(-\beta\Delta E_f/2) \ , \tag{32}$$

where the factor 2 on the RHS reflects the number of the boundaries. This result holds for Neumann boundary conditions; other boundary conditions can be treated in an analogous manner. If the sample consists of N_b independent grains separated by (Neumann type) boundaries, the rate (32) has to be replaced by $r_b \mapsto N_b r_b = L\rho_b r_b$, where ρ_b is the density of grains.

In the presence of impurities, on the other hand, the stability eigenvalue problem yields

$$D(0) = 1 - qF'/2 \tag{33}$$

for the solution (9), and for (10)

$$D(0) = -\frac{F(\hat{\phi}_2 + FF'/4)}{2qg^2}\exp(-2x_{\rm im}/q) \ . \tag{34}$$

From Eqs. (26), (33), and (34) the static prefactor $S_{\rm im}$ for a single impurity follows immediately. In particular, one finds

$$S_{\rm im} = \sqrt{\frac{2qg^2\,(1-qF_m'/2)}{F_s\,(\hat{\phi}_2 + F_sF_s'/4)}}\exp(x_{\rm im}/q) \ , \tag{35}$$

if $F < -2qg$. On the other hand, if $F_c > F > -2qg$, both $D_m(0)$ and $D_s(0)$ are given by Eq. (34). We mention that to $O(F)$ the result (35) can be obtained alternatively by multiplying Eq. (27) with $\lambda_B/\lambda_{\rm pin}$ with $\lambda_{\rm pin}$ from Eq. (17). With the help of the previous results the rate for the nucleation of a KAP at a single impurity is

$$r_{\rm im} = \frac{\lambda_{\rm im}}{2\pi}\,S_{\rm im}\exp(-\beta\Delta E) \ , \tag{36}$$

where $\lambda_{\rm im}$ is the positive solution of Eq. (18). In the presence of impurities with a dilute density $\rho_{\rm im} \equiv N_{\rm im}/L$ ($\ll 1/2x_{\rm im}$), the rate becomes $L\rho_{\rm im}r_{\rm im}$.

V. THE CROSSOVER FROM HETEROGENEOUS TO HOMOGENEOUS NUCLEATION

In a sample consisting of grains each containing a dilute density of impurities, the critical nucleus can be generated by fluctuations in different ways, namely, pinned at an impurity, at a grain boundary, or in a uniform part of the bulk. Consequently, the total rate becomes

$$r_{\rm tot} = (1 - \rho_{\rm im}2x_{\rm im} - \rho_b 2x_f)r_f + N_b r_b + N_{\rm im}r_{\rm im} \ , \tag{37}$$

where the reduction of the effective length available for nucleation of free KAP's has been taken into account. From Eq. (37) the question about the relevant part of the total rate arises. In order to discuss the crossover between homogeneous and heterogeneous nucleation, we

compare the individual rates.

The crossover from boundary to bulk nucleation occurs at the characteristic system size L_c defined by $r_f = r_b$:

$$L_c = 2\sqrt{\frac{\pi\sqrt{1+q^2}\,(1+x_f/q)}{\beta\Delta E_f}} \times \exp(-x_f/2q)\,\exp(\beta\Delta E_f/2)\ . \tag{38}$$

The length L_c is exponentially large for very small noise strengths; in this case nucleation is localized with a large probability at the boundaries of the sample, provided the impurities in the bulk are not relevant. From Eq. (38) the crossover density of grains in a "powder" follows immediately from $(1-\rho_b^c 2x_f)r_f = \rho_b^c L r_b$:

$$\rho_b^c = (L_c + 2x_f)^{-1} \propto L_c^{-1}\ , \tag{39}$$

being valid as long as $L_c \gg 2x_f$.

A crossover density $\rho_{\rm im}^c$ of impurities can be defined in a similar way. From $(1-\rho_{\rm im}^c 2x_{\rm im})r_f = \rho_{\rm im}^c L r_{\rm im}$ it follows that

$$\rho_{\rm im}^c = \frac{\rho_{\rm im}^0}{1+\rho_{\rm im}^0\,2x_{\rm im}}\ , \tag{40}$$

where, e.g., for $F_m < -2qg$,

$$\rho_{\rm im}^0 = \frac{\lambda_f}{\lambda_{\rm im}}\sqrt{\frac{\beta}{2\pi}\frac{F_s(\hat\phi_2 + F_s F_s'/4)}{(1-qF_m'/2)}} \times \exp\{(x_f - x_{\rm im})/q\}\,\exp(\beta\Delta E_{\rm im}) \tag{41}$$

is small for negative pinning energy $\Delta E_{\rm im}$ and large β; hence $\rho_{\rm im}^c \approx \rho_{\rm im}^0$. If $\rho_{\rm im} \approx (2x_{\rm im})^{-1}$, the interaction of a nucleus with more than one impurity becomes important and the result (41) is no longer correct.

We will not discuss here the crossover from boundary nucleation to impurity nucleation, which can be done easily by comparing $\rho_b r_b$ with $\rho_{\rm im} r_{\rm im}$. We only notice that for sufficiently large β boundary nucleation is preferred as long as $\Delta E_{\rm im} > -\Delta E_f/2$.

VI. EXAMPLES

The previous analytical results for the nucleation rate of KAP's at impurities can be further evaluated, once the function $F(\phi)$ is given. Unfortunately, even the qualitative form of an impurity force is usually not known. Nevertheless, it is instructive to consider simple examples. It should be clear that whether heterogeneous nucleation becomes important depends mainly on the change of the activation energy caused by the impurity. In the following, we study first the case of a constant force and then the effect of a coupling of the order-parameter field to the impurity by means of an explicit dependence of F on ϕ.

The most simple type of an impurity is given by a constant force $F(\phi) \equiv F$ independent of ϕ. For a weak force, $|F| \ll 1$, a projection of Eq. (1) onto the translational Goldstone mode $\partial_x\phi(x-x_0)$ of the free critical nucleus yields an ordinary differential equation for the collective coordinate x_0:

$$\dot x_0 = \frac{F}{||\partial_x\phi||^2}\,\frac{d}{dx_0}\phi(x_0)\ . \tag{42}$$

This equation describes the motion of an overdamped particle in a potential proportional to $\phi(x_0)$. Obviously, the only stationary state is given by $x_0 = 0$. Pinning requires $F > 0$, implying also a decrease of the activation energy (see Figs. 4 and 6 below). By using $U = -F\phi$ and $F' \equiv 0$, from the results of Secs. IV and V the activation energy, the static prefactor, the rate, and the density $\rho_{\rm im}^c$ are obtained for arbitrary positive F. For $0 < F < -2qg$ the results follow directly from Eqs. (20), (35), and (41). In the range $F_c > F > -2qg$, on the other hand, the static prefactor reads

$$S_{\rm im} = \exp\{(x_{\rm im}^s - x_{\rm im}^m)/q\} \tag{43}$$

and at the saddle-node bifurcation $F = F_c$ where the metastable and the unstable state collide, one finds $S_{\rm im} \to 1$ since $x_{\rm im}^s \to x_{\rm im}^m$. The activation energy is given by

$$\Delta E = \frac{1}{4}(x_{\rm im}^s - x_{\rm im}^m)F_c^2 - \hat\phi_2^s F \tag{44}$$

and vanishes at $F = F_c$, as one expects. The activation energy ΔE, the size $x_{\rm im}$, and the inverse prefactor $S_{\rm im}^{-1}$ are plotted in Fig. 4 as functions of the impurity force. In order to see how the bifurcation diagram is changed by an impurity, the spatial average $\phi_{\rm ave} = L^{-1}\int dx\ \phi(x)$ of the field $\phi(x)$ is chosen as the order parameter. Figure 5 illustrates the shift of the saddle-node bifurcation at $g = 0$ for different strengths of impurity forces. The equations of state associated with Eqs. (9) and (10), respectively, are $\phi_{\rm ave} = \hat\phi_1 + q^2F/L$ and $\phi_{\rm ave} = \hat\phi_1 + \{(x_{\rm im}+q)\sqrt{1+q^2}F_c - F\}/L$. The stability eigenvalues $\lambda_m^{(0)}$, $\lambda_s^{(0)}$, and $\lambda_s^{(1)}$ are plotted in Fig. 6 as functions of the impurity force. As long as $0 < F < -2qg$, the largest stability eigenvalue of the metastable state remains constant: $\lambda_m^{(0)} = -q^{-2}$. For larger F this eigenvalue grows and becomes zero at the saddle-node bifurcation where it merges with the largest

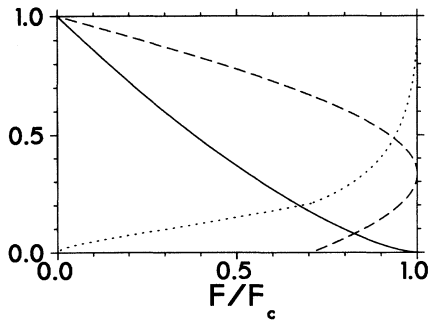

FIG. 4. Properties of the metastable state and the critical nucleus [constant impurity force $F(\phi) \equiv F$; $q = 1$, $g = -0.2$]: $\Delta E/\Delta E_0$ (solid), $x_{\rm im}/x_f$ (dashed), $S_{\rm im}^{-1}$ (dotted). $x_{\rm im}^m = 0$ for $F < -2gq$; $x_{\rm im}^m \to x_{\rm im}^s$ at the saddle-node bifurcation $F = F_c$.

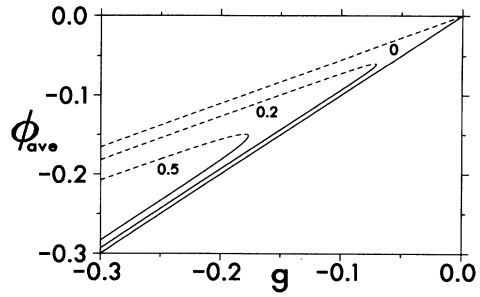

FIG. 5. Shift of the saddle-node bifurcation of the critical nucleus (dashed) and the metastable state (solid) caused by an impurity with constant force $F(\phi) \equiv F$ for various values of F. Order parameter: the spatial average $\phi_{\rm ave}$ of $\phi(x)$; $L = 30$.

eigenvalue $\lambda_s^{(0)}$ of the saddle. The decrease of $\lambda_s^{(1)}$ associated with the translation mode at $F = 0$ reflects the increase of pinning.

The nucleation rates r_f, r_b, $r_{\rm im}$, and $r_{\rm tot}$ are plotted as functions of the inverse noise strength in Fig. 7, which illustrates qualitatively the crossover between heterogeneous and homogeneous nucleation.

In order to study the effect of the coupling of the order parameter to the impurity, we consider the impurity force $F \equiv \varepsilon\phi$. For small $|\varepsilon|$ one can again project the impurity force onto the translational Goldstone mode of the free nucleus and obtain for the collective coordinate x_0

$$\dot{x}_0 = \frac{\varepsilon}{2||\partial_x\phi||^2}\,\frac{d}{dx_0}\left[\phi^2(x_0)\right] \quad . \tag{45}$$

This equation describes an overdamped particle moving in the potential $\propto \phi^2$. There exist three stationary solutions close to the impurity: $x_0 = 0$ and $\pm x_f$. If $\varepsilon > 0$, the potential consists of two hills at $\pm x_f$; hence the impurity is attractive for $|x_0| < x_f$ and repulsive for larger distances. Thus, a saddle is given by the nucleus centered at the impurity; it can be shown to have less energy than the free nucleus (i.e., $|x_0| \gg x_f$) if $q < \sqrt{3}$.

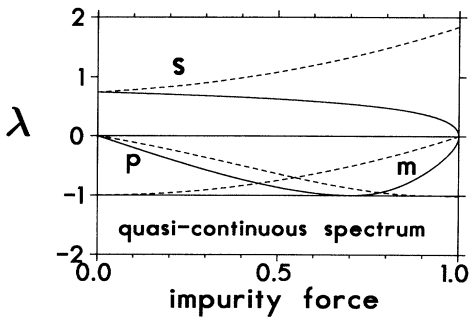

FIG. 6. Stability eigenvalues of states pinned at an impurity: unstable mode $\lambda_s^{(0)}$ (s) and first stable mode $\lambda_s^{(1)}$ (p) of the critical nucleus, first stable mode $\lambda_m^{(0)}$ (m) of the metastable state. Solid curves: $F(\phi) \equiv F$, $q = 1$, $g = -0.2$, scale of x axis F/F_c. Dashed curves: $F(\phi) \equiv \varepsilon\phi$, $q = 1$, scale of x axis $\varepsilon/\varepsilon_c$.

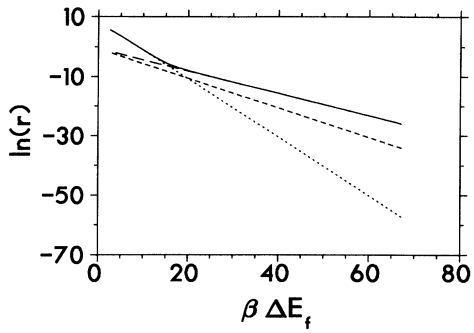

FIG. 7. Dependence of the nucleation rate on $\beta\Delta E_f$ in a grain of length $L = 10^4$ containing a single impurity with constant force $F(\phi) \equiv 0.49$. For very weak noise, the total rate $r_{\rm tot}$ (solid) is dominated by nucleation at an impurity, $r_{\rm im}$ (long-dashed); without impurities the nucleation at the boundaries dominates (short-dashed). For sufficiently large noise homogeneous nucleation r_f (dotted) becomes relevant. ($q = 1$, $g = -0.2$.)

On the other hand, if $\varepsilon < 0$ the stationary points $\pm x_f$ are the saddles, whereas for $x_0 = 0$ both amplitude and translational mode have positive growth rates. In the following $\varepsilon > 0$ is assumed. For arbitrary positive ε the self-consistency condition mentioned in Sec. III implies the amplitudes

$$\phi_m(0) = \frac{\tilde{\phi}_1}{1 - \varepsilon q/2} \quad , \tag{46}$$

$$\phi_s(0) = \frac{\tilde{\phi}_2}{1 + \varepsilon^2/4}\left[1 + \sqrt{1 + q^2(1 + \varepsilon^2/4)}\right] \quad , \tag{47}$$

and the size $x_{\rm im} = x_f - \arcsin(\varepsilon\phi_s(0)/F_c)$ turns out to be independent of the control parameter g. The metastable solution exists only if $\varepsilon < \varepsilon_c \equiv 2/q$; at ε_c the amplitude $\phi_m(0)$ "explodes" and the pinning energy $\Delta E_{\rm im}$ becomes infinite, $\Delta E_{\rm im} \approx 4q^2g^2/(\varepsilon_c - \varepsilon) + O(1)$.

Intuitively one expects that for positive ε the impurity force $F(\phi) = \varepsilon\phi$ tends to destabilize a state. Indeed, one finds an increase of the largest stability eigenvalues belonging to symmetric modes, as shown in Fig. 6. For example, $\lambda_m^{(0)} \approx (\varepsilon/2)^2 - (\varepsilon_c/2)^2 + O(\varepsilon/L)$. Similarly, the eigenvalue $\lambda_s^{(0)}$ associated with the unstable mode of the critical nucleus increases with ε. On the other hand, $\lambda_{\rm pin}$ is shifted to negative values, which indicates pinning.

An interesting property is that the pinning energy can depend nonmonotonically on ε. It is easy to show that for $q < \sqrt{3}$ a finite interval of ε exists where $\Delta E_{\rm im} < 0$, and where thus heterogeneous nucleation at impurities is expected to dominate. The rate is maximal at the local minimum obeying $U_m = U_s$, i.e., $\varepsilon_{\rm min} = (3 - q^2)/2q$. In Fig. 8 the pinning energy is shown as a function of ε for various values of q.

This short discussion illustrates that the effect of impurities on nucleation depends strongly on the specific interaction of the impurity with the order-parameter field. In other words, microscopic details (i.e., specific properties of pinning impurities) play an important role concerning the type of nucleation.

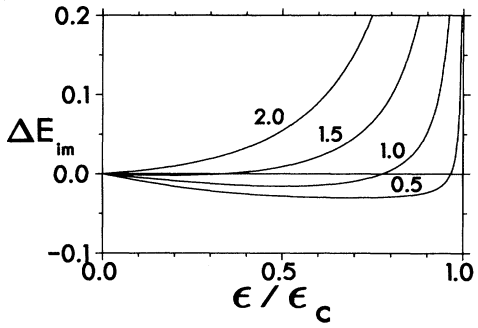

FIG. 8. Pinning energy $\Delta E_{\rm im}$ of an impurity with the force $F(\phi) \equiv \varepsilon\phi$ for various values of q. For $q < \sqrt{3}$ there exists a finite range of ε where $\Delta E_{\rm im} < 0$ implying heterogeneous nucleation.

VII. SUMMARY

In this paper we studied the effects of the finite sample size and of the presence of dilute pointlike impurities on the nucleation rate of kink-antikink pairs in a strongly supersaturated metastable state. Considering a reaction-diffusion equation with a piecewise linear nonlinearity and Neumann boundary conditions, we derived the rates for homogeneous and heterogeneous nucleation. The results could be expressed analytically for an arbitrary impurity force function $F(\phi)$ of the order-parameter field. The comparison of the rates yield the critical sample length L_c and the critical impurity density $\rho_{\rm im}^c$ associated with the crossover between the different kinds of nucleation. Due to lacking translational invariance and the lower activation energy of a nucleus at the boundary compared to that of a free nucleus, L_c turns out to be proportional to $(\beta\Delta E_f)^{-1/2}\exp(\beta\Delta E_f/2)$. If the sample consists of an array of autonomous grains, L_c^{-1} can be interpreted as the density of grains associated with the crossover between homogeneous and grain-boundary nucleation. The comparison of homogeneous and impurity nucleation similarly yields $\rho_{\rm im}^c \propto \sqrt{\beta}\exp(\beta\Delta E_{\rm im})$. Besides the change in the activation energy a generic pinning impurity is able to lower the critical value of the control parameter. Finally, we have illustrated the strong dependence of the results on the specific properties of the impurity (i.e., its coupling to the order-parameter field).

ACKNOWLEDGMENTS

I am very grateful to H. Thomas, F.J. Elmer, P. Talkner, and St. Weigert for helpful discussions. This work was supported by the Swiss National Science Foundation.

[1] J.D. Gunton, M. San Miguel, and P.S. Sahni, in *Phase Transitions and Critical Phenomena*, edited by C. Domb and J.L. Lebowitz (Academic, London, 1983), Vol. 8, pp. 267–428.
[2] S.W. Benson, *The Foundations of Chemical Kinetics* (McGraw-Hill Book Company, New York, 1969).
[3] G. Veser, P.A. Thiel, and R. Imbihl, J. Phys. Chem. **98**, 2148 (1994).
[4] E. Schöll, in *Nonequilibrium Phase Transitions in Semiconductors,* edited by H. Haken, Springer Series in Synergetics Vol. 35 (Springer-Verlag, Berlin, 1987).
[5] K.M. Mayer, R.P. Huebener, and U. Rau, J. Appl. Phys. **67**, 1412 (1990).
[6] H. Malchow and L. Schimansky-Geier, *Noise and Diffusion in Bistable Nonequilibrium Systems,* Teubner Texte zur Physik Band 5 (Teubner-Verlag, Berlin, 1985).
[7] M.C. Cross and P.C. Hohenberg, Rev. Mod. Phys. **65**, 851 (1993).
[8] P. Hänggi, P. Talkner, and M. Borkovec, Rev. Mod. Phys. **62**, 251 (1990).
[9] J.S. Langer, Ann. Phys. (N.Y.) **54**, 258 (1969).
[10] R. Landauer and J.A. Swanson, Phys. Rev. **121**, 1668 (1961).
[11] T. Ohta, Prog. Theor. Phys. Suppl. **99**, 425 (1989).
[12] M. Büttiker and R. Landauer, Phys. Rev. A **23**, 1397 (1981).
[13] P. Hänggi, F. Marchesoni, and P. Sodano, Phys. Rev. Lett. **60**, 2563 (1988).
[14] A.Vl. Gurevich and R.G. Mints, Rev. Mod. Phys. **59**, 941 (1987).
[15] Y. Pomeau, Physica D **23**, 3 (1986); M. Büttiker and H. Thomas, Phys. Rev. A **37**, 235 (1988).
[16] K. Kawasaki and T. Ohta, Physica A **116**, 573 (1982).
[17] E. Meron, Phys. Rep. **218**, 1 (1992).
[18] M. Büttiker and H. Thomas, Phys. Rev. A **24**, 2635 (1981).
[19] S. Coleman, in *Proceedings of the 1977 International School of Subnuclear Physics, Erice, Trapani, Sicily, 1977,* edited by A. Zichichi (Plenum Press, New York, 1979).
[20] T. Christen, Z. Naturforsch. Teil A **48**, 636 (1993).